ELSEVIER

Journal of Alloys and Compounds 239 (1996) 150–157

Journal of ALLOYS AND COMPOUNDS

Anisotropic magnetization of some ferromagnetic and canted transition metal pnictides

H.J. Kohnke, Ch. Kleeberg, V. Dankelmann, K. Bärner*, J.W. Schünemann[1]

4. Physikalisches Institut der Universität Göttingen, Bunsenstr. 13–15, D-37073 Göttingen, Germany

Received 6 October 1995; in final form 15 January 1996

Abstract

The anisotropic magnetization of some $Cr_xMn_{1-x}Sb$ and $MnAs_{1-y}P_y$ single crystals has been measured for temperatures 10 K $< T <$ 500 K and magnetic fields 0 T $< B <$ 0.6 T. From the measurements on the ferromagnetic compounds, the anisotropy constants at different temperatures have been extracted; in one case ($x = 0.05$) two spin reorientation temperatures have been observed ($T_{S1} = 355$ K, $T_{S2} = 523$ K) for $T < T_c = 592$ K. For canted $Cr_{0.4}Mn_{0.6}Sb$ the anisotropy constants are smaller by a factor of 2 to 3, while T_{S1} is increased (453 K).The anisotropy constants for helical $MnAs_{0.94}P_{0.06}$ could not be determined, but its initial susceptibility is anisotropic with $\chi_\parallel/\chi_\perp = 4.4$.

Keywords: Transition metal pnictides; Magnetization; Anisotropy

1. Introduction

The magnetism of metallic transition metal pnictides has been connected with a coupling of the atomic magnetic moments through the conduction carriers in addition to superexchange via the valence band [1,2]. If both couplings are balanced, canted, spiral or random spin structures appear [2]. As the superexchange and the free carrier double exchange coupling are interactions of different quality [2,3], and as this could also lead to spin–orbit interactions of different quality, in this contribution we look for anomalies in the magnetocrystalline anisotropy of various magnetically ordered compounds of this type. In particular, we investigate the magnetic anisotropy of those $Cr_xMn_{1-x}Sb$ and $MnAs_{1-y}P_y$ mixed single crystals which contain canted or helical spin structures, i.e. $Cr_{0.4}Mn_{0.6}Sb$ [4] and $MnAs_{0.94}P_{0.06}$ [2] and that of the ferromagnetic compounds which are close, i.e. $y =$ 0.03, 0.15 and $x = 0$, 0.05, 0.1. We observe anomalies such as a broadening of the angular dependences $M(\theta)$ in certain temperature ranges and double zero crossings of some anisotropy constants K_i. These anomalies, however, might also be connected with the Mn-displacement disorder which is intimately connected with the spin order: displacements of the Mn-ions in the basal plane transform the hexagonal unit cell of the NiAs-type structure into an orthorhombic unit cell; if all displacements are in the same direction we have a uniaxial displacement ("u"). There are, however, three equivalent displacements of this kind possible, and if all three displacements occur randomly on going along an arbitrary crystal direction, then this is called displacement disorder ("rd") [5–7]. According to the phase diagrams of Figs. 1(a) and 1(b), the random displacements can coexist with a spin-glass-like spin order (sg, rd, $T_c < T < T_f$), which should show no global magnetocrystalline anisotropy, as well as with ferromagnetism (fm, rd), for example $x = 0.05$ for $T > 458$ K and $y = 0.15$ for $T < T_c$; in that case we expect only a reduced magnetocrystalline anisotropy compared with the ferromagnetic order under uniaxial displacements (fm, u), for example $x = 0.05$ for $T < 458$ K and $y = 0.03$ for $T < T_u$.

2. Experimental

2.1. Sample preparation

The samples were prepared using the Bridgeman–Stockbarger method as described in detail elsewhere

* Corresponding author.

[1] Lorenz Meßgerätebau, Bundesstr. 116, D-37191 Katlenburg-Lindau, Germany.

0925-8388/96/$15.00 © 1996 Elsevier Science S.A. All rights reserved
PII S0925-8388(96)02220-7

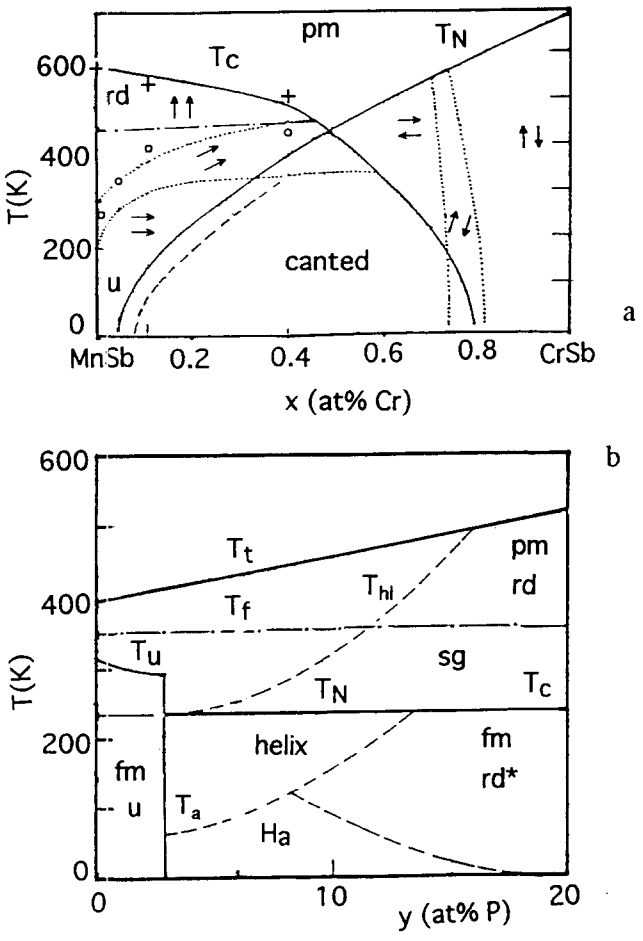

Fig. 1. (a) MnSb–CrSb and (b) MnAs–MnP magnetic phase diagrams according to Refs [20,21]. "u", uniaxial hexagonal–orthorhombic displacement; "rd", random displacements; "rd*", partially random displacements; "pm", paramagnetic state; "sg", spin-glass-like state; "fm", ferromagnetic order; "H_a", helical order along the a-axis; "canted", canted spin order; o, spin reorientation transition temperature T_s; +, Curie temperature T_c; T_N, Néel temperature; T_u, first order transition to fm; T_t, distortive transition; T_{hl} high spin low spin transition; T_a magnetic order–order transition; T_f spin-glass-like transition; ----- dashed line: order–order transition line at $B \approx 0.3$ T [12].

[9,10]. For the measurement of the anisotropy constants, sample disks were cut with the plane normal perpendicular to the c_h- and one a_h-direction. From the disk geometry the demagnetization factor was calculated according to Ref. [11], with the external field B_0 in the plane. The magnetic moment M was measured using a Faraday balance; the magnetic field direction was perpendicular to the field gradient and rotated in the plane by the angle θ, as described elsewhere [12,13]. Curie temperatures and saturation magnetizations coincide well with Refs. [2,4].

3. Results

3.1. $Cr_xMn_{1-x}Sb$ single crystals

Fig. 2(a(II)) shows the magnetization versus temperature curves $\mu(T)$ of $x = 0.4$, $x = 0.1$ and $x = 0$, and Fig. 3(a) some magnetization versus field curves for the easy and hard directions after consideration of the demagnetization, $\mu(H_i)$. Fig. 4(a) shows the angular dependence $M(\theta)$ for $x = 0$ at 210 K as an example. Note that the curvatures of $\mu(\theta)$ around the easy and hard directions are different. Fig. 5 shows Sucksmith plots [14] for $x = 0.4$ and $x = 0.05$ with the intention of separating the anisotropy constants K_1 and K_2. Note that a linear dependence is obtained only for larger fields and that the initial behaviour of $H/M(M)^2$ is opposite for $T = 260$ K and $T = 110$ K ($x = 0.4$). Fig. 6(a) shows the anisotropy constants $K_1(T)$ and $K_2(T)$ for $x = 0.05$, 0.1 and $x = 0.4$, as separated by the Sucksmith procedure. Fig. 6(a), $x = 0.05$, suggests two zero crossings for $K_1(T)$ and $K_2(T)$, i.e. two spin reorientation transitions, as found for MnSb [13]. For $x = 0.1$ and $x = 0.4$ only one spin reorientation temperature T_{S1} is observed as the first zero crossing shifts to higher temperatures with increasing x and as the measurements are limited to $T < 500$ K.

3.2. $MnAs_{1-y}P_y$ single crystals

Fig. 2(a(I)) shows $\mu(T)$ for the ferromagnetic compound $y = 0.03$ and Fig. 2(b) shows $\mu(T)$ for the helically ordered alloy $y = 0.06$ and for the complex ferromagnet $y = 0.15$. $MnAs_{0.97}P_{0.03}$ loses ferromagnetism in a first order transition (temperature hysteresis: $T_{ch} - T_{cc}$); this compound is also very close to (helical) antiferromagnetic order (see Fig. 1(b)) and this leads to an unusual phenomenon: while, during the first cooling, ferromagnetism is not installed, on first heating, at a temperature $T_m < T_{ch}$, $\mu(T)$ suddenly rises steeply. After that initial conditioning $\mu(T)$ is retraced in every cycle. Apparently, the $MnAs_{0.97}P_{0.03}$ single crystal is initially in a helical metastable state.

$\mu(T)$ of the helix is shown in Fig. 2(b(I)); at first sight the anisotropy seems to vanish at the loss of afm long range order (at T_N), however, a closer look reveals a small residual anisotropy up to 300 K (Fig. 4(b(II))). At low temperatures, an order–order transition is indicated at T_a (see also Fig. 1(b)). T_a is even more pronounced for the complex ferromagnet $y = 0.15$. Here $\mu(T)$ is different for cooling in a constant field and for zero field cooling (1,2), suggesting a random spin component; this component, however, is not strong enough to eliminate the anisotropy to the extent found for the spin-glass-like region ($T_N < T < T_f$). Fig. 3(b) shows the $\mu(H_i)$ curves for $y = 0.03$ at 100 K for both the easy and hard directions; here saturation is reached for the easy direction and K_1 and K_2 could be separated for all temperatures. For $y = 0.06$ (helix), saturation was not reached with the fields available, but a significant anisotropy occurs. This can be seen more directly from the $\mu(\theta)$ curves of $y = 0.06$ at 10 K (Fig. 4(b(II))). No notable difference in the

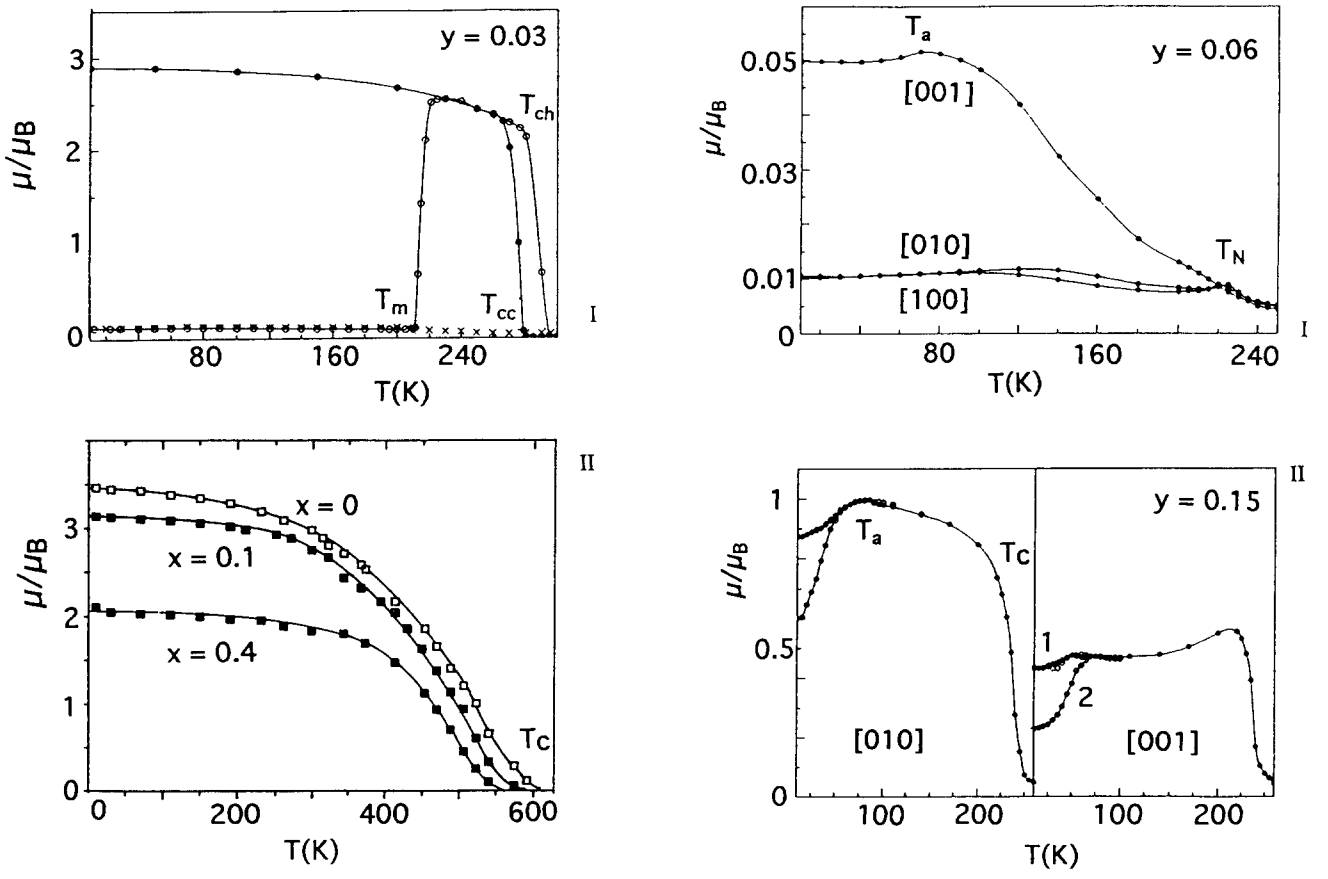

Fig. 2. (a) Magnetization versus temperature curve $\mu(T)$ of an $MnAs_{0.97}P_{0.03}$ single crystal (I) and of some $Cr_xMn_{1-x}Sb$ polycrystals ($x = 0$, 0.1, 0.4) (II); T_m initiation of fm, $T_{cc} - T_{ch}$ hysteresis of the first order transition to fm. (b) $\mu(T)$ of a $y = 0.06$ and a $y = 0.15$ single crystal. Lattice directions in hexagonal notation.

curvatures of $\mu(\theta)$ around the easy and hard directions occurs here; however, this could still happen at higher magnetic fields. At 300 K the anisotropy is much smaller and the easy axis has changed; this indicates another–likely random–spin state for $T > T_N = 220$ K. In contrast, for $y = 0.03$ (Fig. 4(a)), the broadening of $\mu(\theta)$ near the easy direction is obvious. The symmetric curve at the bottom (77 K) refers to the metastable afm state.

The results of the Sucksmith plots, $K_1(T)$ and $K_2(T)$ and the sum $K_1 + K_2$, are depicted in Fig. 6(b) for $y = 0.03$. For higher P-contents, ferromagnetic-like order reappears; this is shown in Fig. 2(b) ($y = 0.15$), while Fig. 4(b) shows $\mu(\theta)$ curves for $x = 0.15$ at different temperatures, which again show the broadening around the easy direction.

4. Discussion

4.1. Anisotropy energy density

According to Fig. 1 and previous work [2], in principle one has orthorhombic symmetry which might degenerate to a quasi-hexagonal symmetry for certain regions of x and T (rd, rd*). However, even in the regions of uniaxial displacements u, the deviations from hexagonal symmetry are rather small [5] and the energy density expression given for hexagonal crystals [15] should be a good approximation:

$$\epsilon = K_o + K_1 \sin^2\theta + K_2 \sin^4\theta + K_3 \sin^6\theta + K_4 \sin^6\theta \cos(6\phi) - H_i M_s \cos\theta \approx K_o + K_1 \sin^2\theta + K_2 \sin^4\theta - H_i M_s \cos\theta \quad (1a)$$

with internal field $H_i = B_o/\mu_o - NM$. As no six-fold symmetry was observed in disks with plane normal parallel to c_h, K_4 can be neglected. Plotting $M(H_i)$ for the easy and hard directions, the energy density ϵ_{eh} can be calculated from the area between the two curves; here, in particular, we obtain the sum of anisotropy constants $\epsilon_{eh} \approx K_1 + K_2$, if K_3 can be neglected too. For a separation of the K_i, the minimum of the free energy density ϵ with respect to θ is set equal to zero and $\cos\theta$ is replaced using $M = M_s \cos\theta$ [14]:

$$H_i/M = 4K_2M^2/M_s^4 - (2K_1 + 4K_2)/M_s^2 \quad (1b)$$

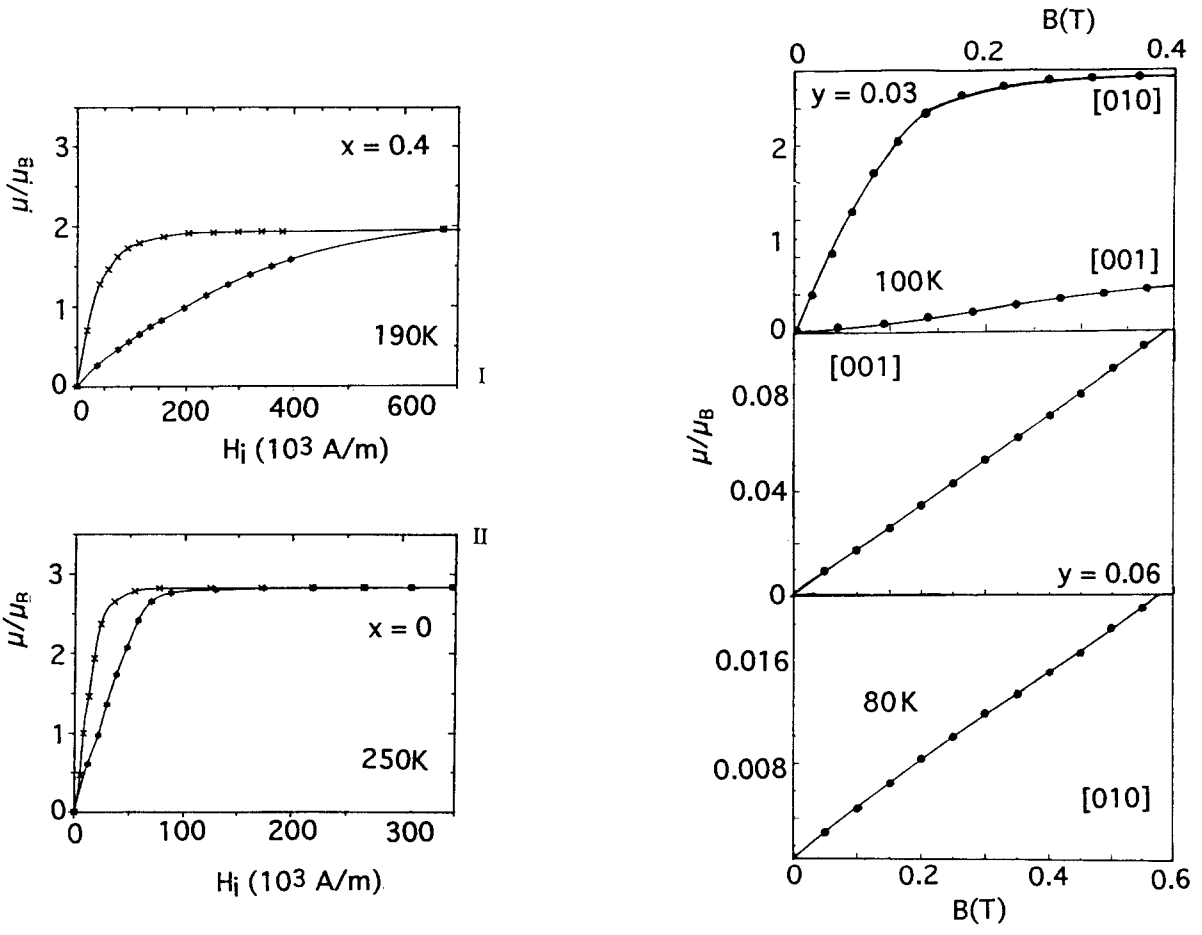

Fig. 3. (a) Magnetization versus internal field curve $\mu(H_i)$ of a single crystal $Cr_{0.4}Mn_{0.6}Sb$ at 190 K and MnSb at 250 K. (b) Magnetization versus external magnetic induction $\mu(B)$ of $MnAs_{0.97}P_{0.03}$ (100 K) and $MnAs_{0.94}P_{0.06}$ (80 K).

Thus, plotting H_i/M versus M^2 (Sucksmith plot), one should obtain a straight line whose slope gives K_2 and whose intercept with the H_i/M axis gives the sum $2K_1 + 4K_2$; i.e. K_1 after subtracting.

Recently, it has been proposed that if an easy cone exists instead of an easy direction (Eqs. (1)), then the energy density should be modified to [13]

$$\epsilon \approx K_0 + K_1 \sin(\theta - \theta_0/2)\sin(\theta + \theta_0/2) + K_2 \sin^2(\theta - \theta_0/2)\sin^2(\theta + \theta_0/2) - H_i M_s \cos(\theta + \theta_0/2) \quad (2a)$$

This reduces to Eq. 1(a) for $\theta_0 = 0$. Using the same procedure as above, for small cone angles $\sin\theta_0/2 \approx 0$ ($\theta_0 < 50°$) one obtains

$$H/M = -(2K_1 + 4K_2^*)/M_s^{*2} + 4K_2^* M^2/M_s^{*4} \quad (2b)$$
$$K_2^* = K_2 \cos^2(\theta_0/2) \quad M_s^* = M_s \cos^2(\theta_0/2)$$

Thus, K_1 can be obtained from a Sucksmith plot but K_2^* is only an effective anisotropy constant as it contains $\cos(\theta_0/2)$; thus, if the slope of the Sucksmith plot changes, it might be connected with changes of the cone angle θ_0. For $x = 0.05$ at 453 K, no cone (Eq. (3)) or canting angle θ_c (Fig. 1(a)) exists and Eqs. (1) should be applicable. Indeed, in the Sucksmith plot deviations from Eq. (1b) are only found for very small fields, i.e. probably the true regime of domain reorientation. For $x = 0.4$, in contrast, the field range of deviations is much larger and the deviation also changes sign with the temperature, suggesting a temperature dependent sublattice canting on an easy cone. Indeed, from neutron diffraction data, $\theta_c = 60°$ lies in the hexagonal plane and is both reduced and rotated into the hexagonal axis with increasing temperature [4].

4.2. Easy cone

The broadening of the curvature of $\mu(\theta)$ near the easy axis in respect to that close to the hard axis at higher fields $B_0 = 0.56$ T (Fig. 4) occurs in both mixed crystal systems. It is likely to be related to an easy cone; for the case of a uniaxial ferromagnet which

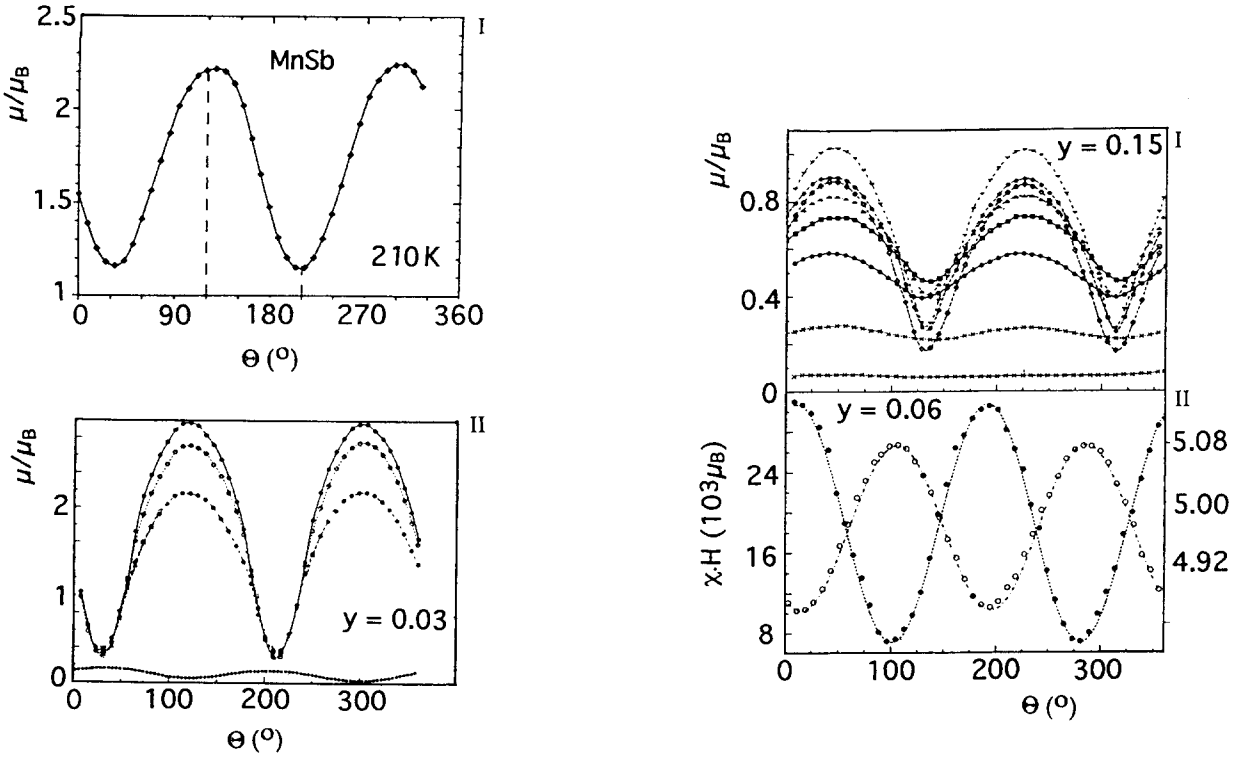

Fig. 4. (a) Angular dependence of the magnetization $\mu(\theta)$ of MnSb at 210 K ($B = 0.06$ T $\parallel c_h$ at 210°) and of $MnAs_{0.97}P_{0.03}$ ($B = 0.58$ T, minimum at [001]) (curves from top to bottom: 10, 200, 280 K, (77 K metastable*). (b) $\mu(\theta)$ for $y = 0.15$ (I), $\chi \cdot H$ for $y = 0.06$ (II). (I) from top to bottom: 50, 100, 150, 200, 220, 230, 240, 250 K, minimum [001], maximum [010], $B = 0.58$ T. (II): ● 10 K, maximum [001]; ○ 300 K.

obeys the condition

$$-2K_2 \leq K_1 \leq 0; \qquad \theta_0 = \arcsin\sqrt{(-K_1/2K_2)} \tag{3}$$

the easy direction spreads out into an easy cone with cone angle θ_0 [16]. $-2K_2$ is indeed lower than $K_1 < 0$, so that condition (3) is fulfilled for all x if $T < T_{S1}$ and for $y = 0.03$ if $T < T_c$. Then from Eq. (3) we obtain $\theta_0 \approx 73°$ for $y = 0.03$–without considering the correction suggested by Eq. (2b). From the equivalence of $\mu(\theta)$ it is reasonable to assume an easy cone also for $y = 0.15$. For $y = 0.06$ there is no such evidence. For the $Cr_xMn_{1-x}Sb$ ferromagnets we have $\theta_0 \approx 50°$, 53° for $x = 0.05$, 0.1 and, if Eq. (3) is also valid for canted structures with a uniaxial symmetry axis of the cant angle, $\theta_0 \approx 53°$ for $x = 0.4$. In this context it might be noted that symmetric $\mu(\theta)$ curves could mean an easy direction, $\theta_0 = 0$, or a regime where the cone characteristics are hidden, i.e. regimes of domain reorientation or spin-glass-like and helical states.

4.3. Anisotropic susceptibility

An anisotropic susceptibility is observed for $y = 0.06$ ($y = 0.08$ [7]) and $T > T_N$, i.e. in the spin random state (sg); however, the easy and hard axes are exchanged as compared with $T < T_N$.

One source for such an anisotropy has been related to the anisotropy of the Lande-factor g [12,17]. For hexagonal symmetry and transformation to the crystal axes the susceptibility tensor should read:

$$\chi = \begin{bmatrix} \chi_\perp & 0 & 0 \\ 0 & \chi_\perp & 0 \\ 0 & 0 & \chi_\parallel \end{bmatrix} \tag{4}$$

this also means a linear dependence $M = \chi H$ for $T > T_N$, as is observed. For the magnetization in the (100) plane, in particular, it follows:

$$M[001] = \chi_\parallel H[\parallel 001] = \chi_\parallel H \sin\phi; \qquad M[010] = \chi_\perp H[\parallel 010] = \chi_\perp H \cos\phi; \qquad \phi \angle B, [010] \tag{5a}$$

assuming that one can reduce any field which lies in the (100) plane to its components. If the susceptibility always measures the field-parallel component, $M(\theta)$ is found to be

$$M(\theta) = M_\parallel = \boldsymbol{M} \cdot \boldsymbol{H}/H = \chi_\parallel \sin^2\phi + \chi_\perp \cos^2\phi \tag{5b}$$

In Fig. 4(b(II)) the experimentally obtained data $\mu(\theta)$ are presented and indeed follow Eq. (5b). $M \sim H$ is

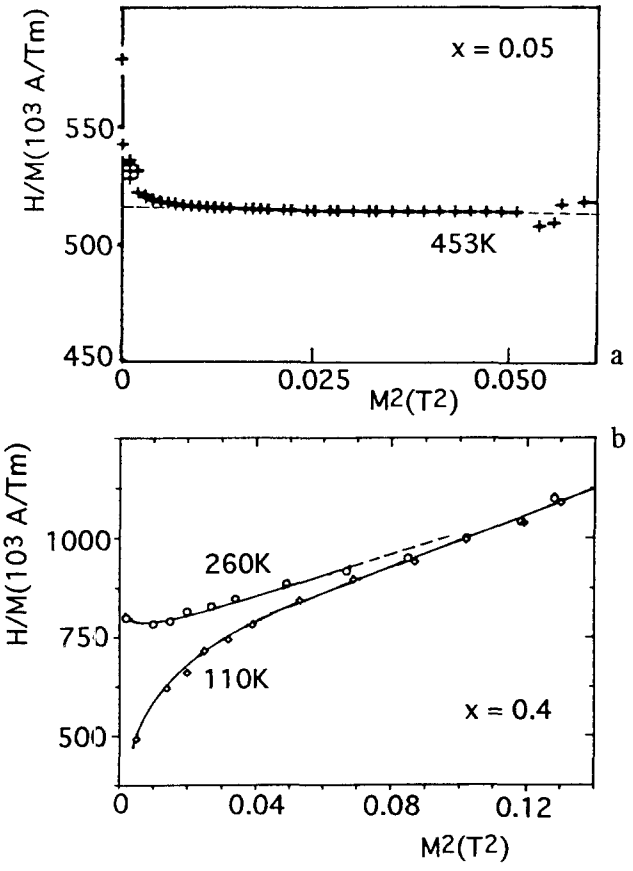

Fig. 5. Sucksmith plots of $Cr_{0.05}Mn_{0.95}Sb$ ($T = 453$ K) and $Cr_{0.4}Mn_{0.6}As$ ($T = 110$, 260 K).

also true for $y = 0.06$ at all temperatures $T < T_N$ and $B < 0.6$ T (H_a-helix); this (initial) susceptibility can also be described by Eqs. (5) (Fig. 4(b)). An H_a-helix is also proposed for $y = 0.15$ at low temperatures and $B = 0$ (Fig. 1), however, $\mu(\theta)$ at 50 K is not described by Eqs. (5) (Fig. 4(b(I))). Close to ferromagnetism, however, the helix can be very easily transformed to a ferromagnetic state, whose anisotropy might involve an easy cone.

4.4. Magnetization curve for a sublattice canting on an easy cone

If one reduces the anisotropy energy density to a uniaxial anisotropy ($K_1 \gg K_2$), approximates the sublattice magnetizations by

$$M_i/M_s \approx \sin(\theta + \theta_o/2 - \theta_c/2) = \sin(\theta + \theta_o^*/2) \qquad (6a)$$

and then equates the angular dependence of the energy density $\partial\epsilon/\partial\theta$ (Eq. (2a) without the Zeeman term) with that of the Zeeman energy $\partial(HM_s\cos(90 - (\theta + \theta_o^*/2))/\partial\theta$ (momentum balance), then one obtains for small angles, $\sin(\theta_o^*/2) \approx 0$:

$$2K_1 \sin\theta\cos\theta = M_s H\cos(\theta_o^*/2)\cos\theta + \ldots;$$
$$M_s = M_{so}\cos(\theta_c/2) \qquad (6b)$$

If the cone stays intact while its axis rotates by θ, from Eqs. (6) and (2), for the $M(H)$ curve we obtain

$$M/M_s(\cos\theta_o^*/2) = (H/H_{ko}^*) + (\tan\theta_o^*/2)\sqrt{[1-(H/H_{ko}^*)^2]};\quad H \leq H_{ko}^*$$
$$H_{ko}^* = 2K_1/M_s\cos(\theta_o^*/2);\quad \theta_o^* = \theta_o - \theta_c \qquad (7)$$

The use of $\theta_o^* = \theta_o - \theta_c$ interpolates rather well between two limiting cases 1, 2: (1) when at $H = 0$ the vector sum $\boldsymbol{M}_1 + \boldsymbol{M}_2$ lies in the easy direction (cone axis at $\theta = 0$ and $\theta_o = \theta_c$) and is rotated against an anisotropy $K_1\sin^2\theta$ under conservation of the cant angle; and (2) the ferromagnetic case, $\theta_c = 0$, where at $H = 0$ the magnetization vector lies on the turning side of the cone. The solution of Eq. (7) is, however, restricted to cone angles $\theta_o^* < 50°$ because of the approximation made in Eq. (6). One example, $\theta_o^* = 40°$ is shown in Fig. 7: for $H \to H_{ko}^*$, Eq. (7) gives $M = M_s\cos\theta_o^*/2$; however, M_s is already reached at a lower field $H_{ko} = 2K_1/M_s$, i.e. when one side of the cone is parallel to the hard direction. The magnetization at zero field, $M(0)$, usually cannot be observed because of domain formation, however, according to Eq. (7), after domain reorientation there should be a downward curvature. For $x = 0.4$, $\mu(H)$ for the hard direction indeed shows a downward curvature for intermediate fields (Fig. 3(a)) and so does $\mu(H)$ of $y = 0.17$ (Fig. 7(b)). If, in particular, the cone and cant angles vanish with increasing external field, the $M(H)$ curve should approach a linear dependence $M/M_{so} = H/H_{ko}$; this is also shown in Fig. 7(a). According to the figure, an upward curvature could be obtained in this way. However, a decreasing sublattice canting could also lead to a change of K_1 and with it H_{ko} as the spin–orbit coupling might change.

4.5. Temperature dependence of the anisotropy constants

If one assumes that small temperature-induced deviations of M from the direction determined by temperature-independent local anisotropy constants k_i

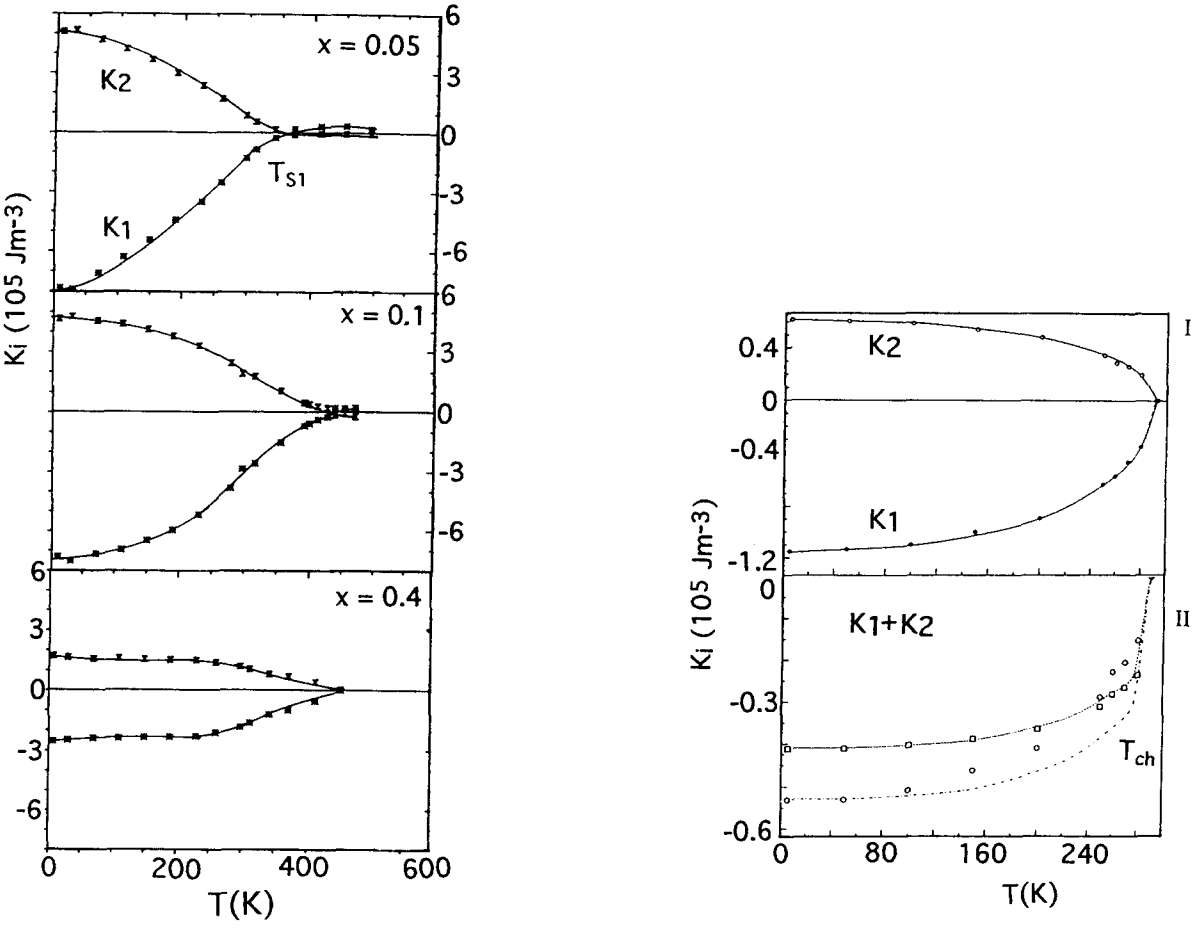

Fig. 6. (a) Anisotropy constants $K_i(T)$ of some $Cr_xMn_{1-x}Sb$ single crystals ($x = 0.05, 0.1, 0.4$); T_{S1} spin reorientation temperature. (b) $K_i(T)$ and temperature dependence of $K_1 + K_2$ for $MnAs_{0.97}P_{0.03}$. ----- theory; □ by summation; ○ by integration of $\mu(H_i)$ curves.

follow a random walk function, one obtains for the macroscopic hexagonal $K_i(T)$ [18,19]:

$$K_1 = (k_1 + 8k_2/7)(M/M_s)^3 - (8k_2/7)(M/M_s)^{10} \quad (8a)$$

$$K_2 = k_2(M/M_s)^{10} \quad (8b)$$

according to Eq. (8), the K_i vanish at $T = T_c$ and are maximal for $T \rightarrow 0$, as is observed for $y = 0.03$ (Fig. 6(b)). A complete fit to the experimentally observed $K_i(T)$ or the sum $K_1 + K_2$ can be made by assuming $K_1/K_2 = k_1/k_2$ not only at $T = 0$ (Eq. (8)) but also at the lowest temperature available (approximately 10 K). This has been done in Fig. 6(b) for $K_1 + K_2$ of $y = 0.03$; the agreement is satisfactory.

The random-walk approach used to derive Eq. (8) does not yield a zero crossing for the $K_i(T)$ for $T < T_c$, such as found for the $Cr_xMn_{1-x}Sb$ single crystals. Accordingly, the original calculations [18,19] have been expanded to include the thermal expansion via the phonon influence on the spin–orbit interaction [20]. To first order this can be written as an expansion of the local anisotropy constants k_i; for example, one may write [20]

$$K_2 = k_{2o}(1 - \alpha T/T_c)(M/M_s)^{10}; \quad T_s = T_c/\alpha \quad (9)$$

the expansion coefficient α is related to the volume thermal expansion $\delta v/v_o$ and would determine the (first) spin reorientation temperature of $Cr_xMn_{1-x}Sb$. A second spin reorientation temperature T_{S2} [21,22], as indicated for $x = 0.05$, cannot be explained this way.

If, however, we were to have a change of the lattice, we could also shift the spin reorientation temperature $T_{S1} \rightarrow T_{S2}$. According to the phase diagram (Fig. 1), the u ↔ rd displacement disorder transition (at 458 K) lies between T_{S1} and T_{S2} and is therefore probably the cause for the occurrence of T_{S2} [13]. Also, the increasingly low values of the anisotropy constants would be consistent with an increasing randomizing of the Mn-displacements.

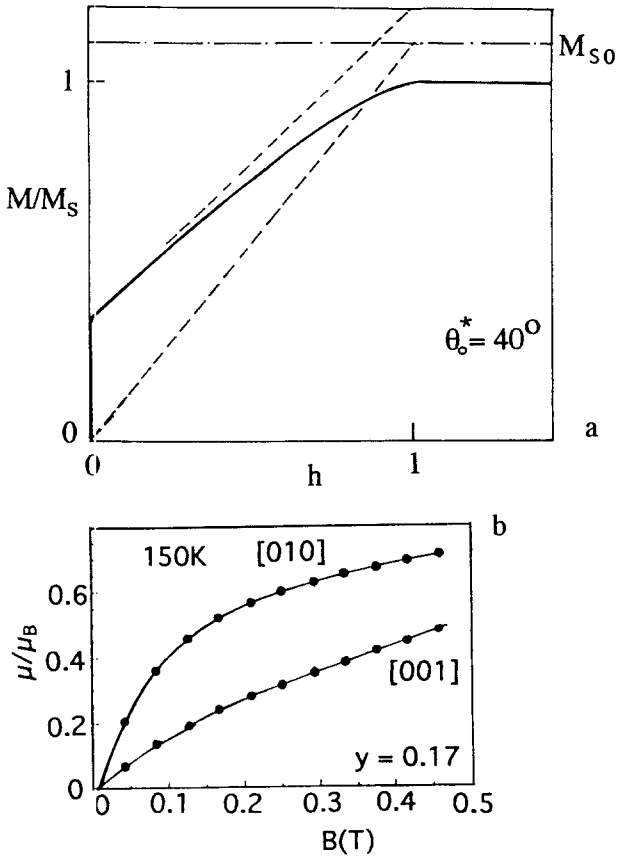

Fig. 7. (a) $M(h)/M_s$ where $h = H/H_{k0}$ as calculated according to Eq. (7) ($\theta_0^* = 40°$). (b) $\mu(B)$ for the easy and hard directions of a $y = 0.17$ single crystal at $T = 150$ K.

5. Conclusions

Random Mn-displacements which occur at higher temperatures are responsible for anomalies in the temperature dependence of the K_i, in particular for the occurrence of a second spin reorientation temperature in $Cr_xMn_{1-x}Sb$ single crystals. Mixed couplings, which are used to explain canted or helical equilibrium spin structures, are probably the cause of the field- and temperature-dependent sublattice cantings and might also be related to the frequent appearance of easy cones.

Acknowledgements

The authors would like to thank the Deutsche Forschungsgemeinschaft for continuous support and P. Mandal and E.A. Zavadskii for helpful discussions. Two of us are also indebted to the Alexander von Humboldt foundation.

References

[1] K. Bärner, *Phys. Status Solidi B, 88* (1978) 13.
[2] H. Fjellvag, A.F. Andresen and K.Bärner, *J. Magn. Magn. Mater., 46* (1984) 29.
[3] P.G. de Gennes, *Phys. Rev., 118* (1960) 141.
[4] W. Reimers, E. Hellner, W. Treutmann and G. Heger, *J. Phys. C, 15* (1982) 3597. [5] G.A. Govor, K. Bärner and J.-W. Schünemann, *Phys. Status Solidi A, 113* (1989) 755.
[6] V. Dankelmann, H.J. Kohnke, J.-W. Schünemann, K. Bärner, S. Buzhinsky and I.V. Medvedeva, *J. Alloys Comp., 209* (1994) 305.
[7] G.A. Govor, A.K. Vecher, Ch. Kleeberg, J.W. Schünemann, V. Dankelmann and K. Bärner, *Phys. Status Solidi A, 138* (1993) 307.
[8] H.J. Kohnke, H. Dunkel, J.-W. Schünemann, K. Bärner and S. Buzhinsky, *Phys. Status Solidi B, 182* (1994) 411.
[9] H.J. Kohnke, *Diploma Thesis*, Göttingen, Germany, 1991.
[10] Ch. Kleeberg, *Diploma Thesis*, Göttingen, Germany, 1993.
[11] J.A. Osborn, *Phys. Rev., 67* (1945) 351.
[12] H. Berg, *Phys. Status Solidi A, 40* (1977) 559.
[13] H.J. Kohnke, V. Dankelmann, Ch. Kleeberg, J.W. Schünemann, K. Bärner, A. Vetcher and G.A. Govor, submitted to *Phys. Status Solidi B.*
[14] W. Sucksmith and J.E. Thompson, *Proc. Roy. Soc. (London), A225* (1954) 362.
[15] W.P. Mason, *Phys. Rev., 96* (1954) 302.
[16] C.R. Chang, *J. Appl. Phys., 69* (1991) 2431.
[17] E.A. Turov, *Physical Properties of Magnetically Ordered Crystals*, Ac. Press, 1965, p. 98 ff.
[18] C. Zener, *Phys. Rev., 96* (1954) 1335.
[19] W.F. Carr, *Phys. Rev., 109* (1958) 1971.
[20] R. Brenner, *Phys. Rev., 107* (1957) 1539.
[21] T. Okita and Y. Makino, *J. Phys. Soc. Jpn, 25* (1968) 120.
[22] G. Markandeyulu and K.V.S. Rama Rao, *J. Magn. Magn. Mater., 67* (1987) 215.